Assessment of Electrical Injection of Corrosion Inhibitor for Corrosion Protection of Reinforced Concrete

Tongyan Pan
Research Engineer, Ph.D., P.E.
Western Transportation Institute
Montana State University
P.O. Box 174250
Bozeman, MT 59717-4250
Tel: (406) 994-6323
Email: tongyan.pan@coe.montana.edu

Tuan Anh Nguyen
Postdoctoral Research Associate, Ph.D.
Corrosion, Electrochemistry and Analysis Laboratory
Western Transportation Institute
Montana State University
P.O. Box 174250
Bozeman, MT 59717-4250
Tel: (406) 994-6114
Email: anh.tuannguyen@coe.montana.edu

Xianming Shi *
Research Scientist II, Ph.D., Western Transportation Institute
Associate Research Professor, Civil Engineering Department
Montana State University
P.O. Box 174250
Bozeman, MT 59717-4250
Tel: (406) 994-6114
Email: xianming_s@coe.montana.edu

* Corresponding author

Paper Revised for Inclusion in the CD-ROM of the TRB 2008 Annual Meeting Committee AHD45: Corrosion

Submission date: Oct. 24, 2007

Abstract

Chloride ingress is the major cause of rebar corrosion that deteriorates reinforced concrete structures in chloride-laden environments. A recently emerged electrochemical technique - the electrical injection of corrosion inhibitor (EICI) - shows its potential in protecting rebar from chloride attack by driving corrosion inhibitors to rebar surface under an externally applied electric field. This paper assesses the potential applicability of EICI as a routine electrochemical treatment for corrosion protection. A comprehensive evaluation of currently available organic cation-based inhibitors was conducted based on the measured corrosion inhibition performance and diffusion coefficient of each inhibitor. Using a two-dimensional finite element model developed by the authors, the concentration evolution of the selected inhibitors and chloride were predicted on rebar surface and in concrete, and the applicability of EICI was examined thereafter. Important aspects of EICI were studied including mainly inhibitor type, magnitude of applied current density, and treatment time. Recommendations regarding the EICI practice were made accordingly.

Introduction

Accelerated corrosion of reinforcing steel is often observed in chloride-laden environments, which leads to premature failure of reinforced concrete structures and shortens their service lives. Such concrete structures include highway concrete slabs and bridge decks exposed to winter deicer/anti-icer applications [1], structures working in marine environments [2-3], etc. Excessive chloride is also introduced into concrete sometimes as admixture, e.g., when calcium chloride is added in fresh concrete as a set accelerator, which was reported to cause premature structural problems related to steel corrosion [4].

Chloride-induced rebar corrosion can be mitigated by reducing the level of chloride ions in concrete via various mechanisms such as electrochemical extraction, thermal accelerated diffusion, and pressurized removal [5-6]. Chloride-induced rebar corrosion can also be effectively mitigated by certain chemicals serving as corrosion inhibitors. Such inhibitors can be admixed into fresh concrete for new structures, or surface-applied if they are volatile organic compounds used to rehabilitate preexisting structures [7], or driven into hardened concrete through an external electric filed. The mitigating mechanism, however, entails a complex electrochemical process that depends primarily on the concentration of chloride ions relative to those of the protective species [8].

The effectiveness of an inhibitor in mitigating chloride-induced corrosion can be determined using laboratory tests that involve exposing a sample rebar to a simulated concrete pore solution that contain the inhibitor and chloride at given concentrations and examining the corrosion rate of rebar over time. Determining the concentrations of the inhibitor and chloride ions on rebar surface and in concrete subsequent to the electrical injection of corrosion inhibitor (EICI), on the other hand, requires efforts in modeling.

In concrete, chloride and inhibitor ions travel via three primary mechanisms: natural diffusion, electric migration, and transport by movement of pore solution due to capillary suction or external pressure gradient [9]. In water-saturated concrete, chloride ions migrate mainly via natural diffusion and electric migration [10]. The natural diffusion of chloride ions depends predominantly on their concentration gradient, which may also be affected by the electric membrane potential formed in concrete [10]. During rebar corrosion, chloride ions could also migrate from local cathodes to local anodes under the electric field generated by the corrosion cell [8]. In contrast to the internally established electric fields mentioned above, an external electric field is often applied to control the transport of chloride ions and protective species in concrete [11-12]. Applications of such electrochemical treatments include mainly the electrochemical realkalization, electrochemical chloride extraction (ECE), cathodic protection, and EICI [11,13,14]. In ECE, an electric field with a current density of 1~5 A/m^2 is usually applied to a concrete structural component for a few weeks, under which chloride ions migrate out of concrete towards the external anolyte solution [11,15]. In cathodic protection, a much lower current density is maintained for decades to prevent the corrosion of rebar in concrete, which also helps prevent excessive accumulation of chloride ions on rebar surface. Using a setup similar to ECE, EICI drives inhibitor ions into concrete (some of which may reach the rebar surface), while at the same time removing chloride ions out of concrete.

The corrosion of steel in concrete consists of electrochemical reactions, an anodic reaction (e.g., iron atoms are oxidized to ferrous cations that then form ferrous oxides/hydroxides) and a cathodic reaction (e.g., oxygen molecules are reduced to hydroxyl anions in presence of water) that progress simultaneously. Chloride ions can act as a catalyst in the anodic reaction of corrosion process once they penetrate the concrete cover and reach a threshold level high enough to disrupt the passive film on rebar surface (typically a ferrous hydroxide layer of nanometers thick). Such depassivation of passive film on rebar surface usually lead to subsequent accelerated corrosion [16-17] if no protective action is taken.

Corrosion inhibitors can be classified into anodic type, cathodic type, or mixed type, depending on their inhibition mechanism. Anodic inhibitors reduce the rate of reaction at the anodic site and they usually react with the corrosion products to form a protective coating on the metal surface. Cathodic inhibitors act indirectly to mitigate corrosion by preventing the reaction at the cathodic site. They are often adsorbed on the steel surface and act as a barrier to the reduction of oxygen. Mixed inhibitors

influence both the anodic and cathodic sites of corrosion, often by forming an adsorbed film to the metal surface. This is especially beneficial in reinforced concrete due to the prominence of micro-cell corrosion.
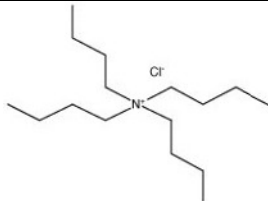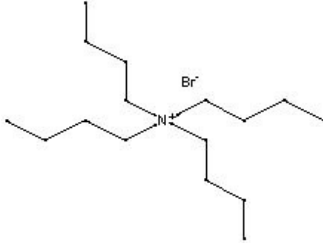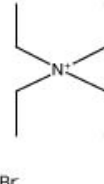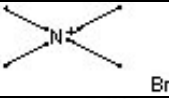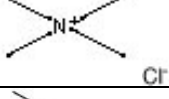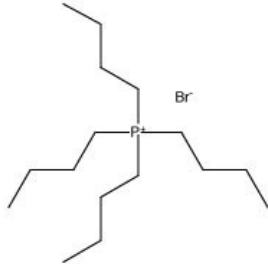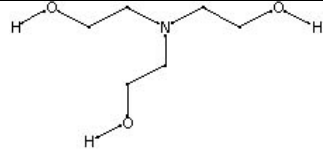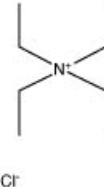
EICI was shown to be an effective method of adding corrosion inhibitors to preexisting structures, which can thus serve as a rehabilitative measure to retard or reduce corrosion. In a SHRP study in 1987 [18], SRI developed *quaternary ammonium* and *phosphonium* corrosion inhibitors that can be electrically injected into concrete matrices. The inhibitors are cationic, i.e., positively charged, and hence conceptually can be applied to concrete structures using the ECE facilities. The study showed that such inhibitor injection could provide adequate corrosion protection to rebars embedded in chloride-contaminated concrete. The technology features its novelty and nondestructive nature, and the requirement of only temporary installation (10-15 days). Although electrical potential and current density as high as 5-10V/cm and 4.6-12.4 A/m^2 respectively were once used [18]; recently the National Association of Corrosion Engineers (NACE) suggests that the applicable current density should not exceed $4A/m^2$ of steel surface area, and that the treatment charge density should not exceed $1500Ah/m^2$. Limited studies have been published since the SHRP study, likely due to the high cost of aforementioned corrosion inhibitors. A recent study investigated the electromigration of two organic base corrosion inhibitors, *ethanolamine* (pK_a 9.5) and *guanidine* (pK_a 13.6) [19]. pKa is their acid-ionization constant. In this EICI process, an electric field was applied between steel embedded in concrete and an external anode, with the cathodic current density galvanostatically controlled in the range 1~5 A/m^2 for 3-14 days. Experiments with the same conditions but without an electric field were also conducted, by applying the corrosion inhibitors to similar saturated concrete surfaces from external electrolyte. The inhibitor concentration profiles indicated that the two inhibitors were effectively injected into carbonated reinforced concretes investigated and their electrical injection in non-carbonated concrete was far less effective. In carbonated concrete, the inhibitors became concentrated near the embedded steel. In non-carbonated concrete (*w/c*=0.65, pH>13), guanidine penetration was accelerated to a modest extent by the applied field but a 2-week, $5A/m^2$ treatment did not cause sufficient inhibitor to reach the rebar at a cover depth of 35mm. Ethanolamine penetration in non-carbonated concrete was not significantly enhanced by the electric field. These findings were explained in terms of the influence of the pH of the concrete pore solution on the degree of ionisation of the organic bases and hence on their tendencies to migrate and neutralise cathodically-generated hydroxyl ions [19].

While ECE and EICI are promising techniques to treat chloride contamination in concrete, more widely applications of them are hindered by the lack of detailed information on the underlying mechanisms and relevant rate-limiting steps. Existing experimental works in this field are far from systematic, although limited experimental information can be coupled with theoretical modeling to improve the understanding of these phenomena. This study in our laboratory aimed at evaluating the effectiveness of various organic chemicals as potential inhibitors for rebar corrosion, and assessing the applicability of EICI as an effective corrosion protection technique. The anti-corrosion effectiveness of the organic cation-based inhibitors was determined based on their inhibition efficiencies over time as evaluated from electrochemical tests. The evolution of the inhibitor and chloride on rebar surface was predicted using a two-dimensional (2D) finite element model developed by the authors.

Experimental Design of Inhibitor Evaluation

For EICI, inhibitors that demonstrate satisfactory inhibition effectiveness, and equally importantly, that can also be electrically driven to the rebar surface in a short time are highly desired. The following sections of this paper summarize the inhibitors selection and evaluation based on these two criteria. Eight organic chemicals in Table 1 were selected as the candidate inhibitors for preliminary evaluation, in terms of their inhibition effectiveness. The best performers were then further evaluated for their electromigration behavior. Note that Table 1 also includes a ninth chemical - the Proprietary Inhibitor - as the intentional pseudonym to a chemical agent that may have commercial value.

Table 1: Nine Candidate Inhibitors Subjected to Laboratory Evaluation

Inhibitor	Chemical Name	Molecular Structure	Abbreviation
#1	Tetrabutylammonium Chloride		TBA-C
#2	Tetrabutylammonium Bromide		TBA-B
#3	Tetraethylammonium Bromide		TEA-B
#4	Tetramethylammonium Bromide		TMA-B
#5	Tetramethylammonium Chloride		TMA-C
#6	Tetrabutylphosphonium Bromide		TBP-B
#7	Triethanolamine		TEOA
#8	Tetraethylammonium Chloride		TEA-C
#9	Proprietary Inhibitor	N/A	PI

Laboratory Evaluation of Inhibitor Effectiveness

The inhibition efficiency (percent reduction in corrosion rate of an inhibitor with respect to the control sample) of the first eight chemicals in Table 1 was tested in our laboratory. A588 steel disc samples were sealed in epoxy, polished to grit size 600, cleaned with acetone and de-ionized water, and dried before being immersed in simulated concrete pore solutions for corrosion testing. The test solutions were adjusted to a pH of 12 using sodium hydroxide, having a sodium chloride concentration of 0.5M to simulate a very aggressive environment. A solution without any inhibitor added was used as control, whereas the other eight solutions had each of the first eight inhibitors added at 20mM. Each of the eight inhibitors and the control solution was tested in three duplicates. For each solution, a three-electrode cell was used for electrochemical testing, consisting of a saturated calomel electrode (SCE) as the reference electrode, a platinum mesh as the counter electrode, and the steel sample with an exposed surface area of 1.4 cm^2 as the working electrode. A Gamry Electrochemical Multiplexer ECM8 was used to monitor the open circuit potential (OCP) of steel samples and to measure their corrosion rate via potentiodynamic weak polarization (-30 to +30 mV vs. OCP at 0.2mV/s). The weak polarization range of -30 ~ +30 mV was adopted to minimize measuring errors of the test instrument; and to prevent potential significant change in the surface state of electrodes, in the solution composition, or in the controlling corrosion mechanism and kinetics. The Gamry analysis software was used to analyze the polarization data. Table 2 presents the average of the three instantaneous corrosion rates of steel in the nine solutions over time.

Table 2: Performance of Eight Inhibitors in Aggressive Chloride Solution

Inhibitor	Corrosion Rate of Steel (MPY)						Average Inhibition Efficiency
	1-hr	24-hr	72-hr	240-hr	Mean	Standard Deviation	
None	1.47	5.71	13.14	3.32	5.91	5.12	N/A
TBA-C	2.69	0.44	0.98	4.50	2.15	1.83	64%
TBA-B	1.10	0.76	1.44	0.19	**0.87**	**0.53**	**85%**
TEA-B	1.58	4.96	1.53	1.04	2.28	1.80	61%
TMA-B	3.04	0.84	0.58	2.05	1.63	1.14	72%
TMA-C	1.21	1.05	1.81	1.91	**1.50**	**0.43**	**75%**
TBP-B	10.01	1.92	0.27	1.32	3.38	4.47	43%
TEOA	0.59	0.55	0.93	13.57	3.91	6.44	34%
TEA-C	1.16	15.90	1.18	1.09	4.83	7.38	18%

As shown in Table 2, the data of average corrosion rate of steel at the four sampling points show that TBA-B and TMA-C outperformed other chemicals as corrosion inhibitors in the simulated concrete pore solution, by reducing the corrosion rate of steel by 85 percent and 75 percent, respectively. The low standard deviations in the corrosion rate of steel in presence of TBA-B and TMA-C further confirmed their good performance as corrosion inhibitors. In absence of inhibitors, the corrosion rates of steel in the control solution were higher than a few millimetres per year, and this high corrosivity of solution can be explained by its high molar ratio of chloride-to-hydroxyl ions (50 in this case).

More laboratory tests were conducted to further investigate the performance of TBA-B and TMA-C in less aggressive environments representative of concrete with less chloride contamination or with reduce chloride content through electrochemical treatment. The test solutions were adjusted to a pH of 13 to simulate typical alkaline environment of hydrated cement concrete, having a sodium chloride concentration of 133 mM and 66 mM to simulate typical free chloride concentration in contaminated concrete with a total chloride concentration of 500 mM and 250 mM respectively.

Table 3: Performance of TBA-B and TMA-C in Mild Chloride Solution

[Inhibitor] (mM)	[Cl⁻] (mM)	Corrosion Rate of Steel, at 48 Hours of Immersion (MPY)		Inhibition Efficiency	
		TBA-B	TMA-C	TBA-B	TMA-C
0	133	0.193	0.193	N/A	N/A
	66	0.131	0.131	N/A	N/A
5	133	0.187	0.041	3.1%	65.6%
	66	0.125	0.045	4.6%	76.7%
50	133	0.104	0.033	46.1%	82.9%
	66	0.048	0.022	63.4%	83.2%

Table 3 gives the corrosion rates of steel at 48 hours of immersion in presence of TBA-B or TMA-C, which can be reasonably used to indicate the anti-corrosion effectiveness of the two inhibitors. The data indicate that TMA-C outperformed TBA-B as corrosion inhibitor in the less aggressive environments. Generally the corrosion of steel was less severe in simulated concrete pore solutions with a lower chloride concentration (66 mM vs. 133 mM), or with a higher inhibitor concentration (50 mM vs. 5 mM and 0 mM). Both inhibitors are likely mixed-type inhibitors, and they reduce corrosion of steel by forming an adsorbed film to the metal surface and thus acting as a barrier to both the chloride attack to iron atoms and the reduction of oxygen. In absence of inhibitors, the corrosion rates of steel in the two control solutions were lower than 0.2 MPY (i.e. mils per year), consistent with their low molar ratio of chloride-to-hydroxyl ions (1.3 and 0.66 respectively, both however exceed the commonly agreed corrosion threshold ratio of 0.60).

Laboratory Determination of Diffusion Coefficients in Concrete

The transport speed of a species in concrete can be effectively characterized by its diffusion coefficient (D). Since the D values of chloride and organic cations are highly dependant on the materials properties of concrete such as chemical composition of cement hydration products and internal structure of concrete matrix, they were measured in this study using electrically-accelerated migration tests.

Figure 1: Laboratory Setup for Measuring the D values of Chloride or Inhibitors

The electro-migration tests of TBA-B and TMA-C were conducted using a two-compartment glass cell that sandwiches a 2-cm thick concrete disc specimen as shown in Figure 1. The concrete specimen used Type I cement and included sand only with the size of 0.85-2 mm. The cement: sand: water ratio by weight was 1:4:0.5. Each fresh concrete sample was carefully compacted. Both sides of the glass cell contain an electrolyte of 400 mM NaOH to simulate concrete pore solution. The inhibitor of interest - TBA-B or TMA-C - was included in the left compartment at 200mM. Using a DC power supply, an electric field of 12 volts was applied to the two ends of the concrete specimen, with two polished glassy carbon electrodes in the left and right compartment serving as the anode and cathode respectively. Sample solution in the right compartment (catholyte) was taken periodically to be analyzed by the UV-Visible Absorbance Spectroscopy, which is a proven technology for accurately detecting organic chemicals in aqueous solutions [20]. By testing five standard 0.4M NaOH solutions of TBA-B with a concentration of 1 mM, 10 mM, 100 mM, 200 mM, and 500mM respectively, a calibration curve was established to correlate the optical density at the characteristic peak (between 220-230 nm wavelength, as shown in Figure 2a) and the inhibitor concentration. The calibration curve was then used to determine the unknown TBA-B concentration of sample catholytes.
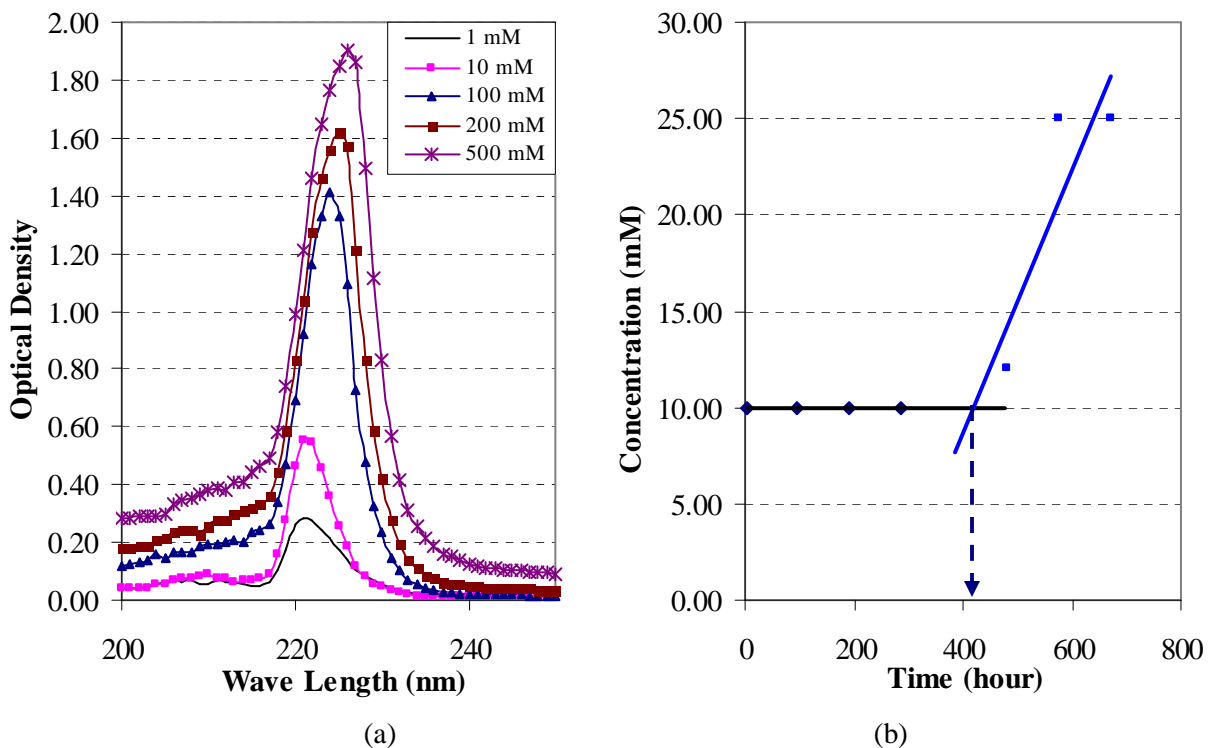

(a)   (b)

Figure 2: (a) UV-Visible Spectroscopy for Five Standard TBA-B Solutions: (b) Determination of the Penetration time t_0 (416 hours) for Inhibitor TBA-B

The values of D of the inhibitors were calculated based on a method derived from Buenfeld et al. [5]. The method was formulated in Equation 1, where t_0 is the time taken for inhibitor ions to penetrate the concrete disc. The magnitude of t_0 was determined by monitoring the inhibitor concentration in the destination solution until a steady state flux, as indicated in Figure 2b by the onset of increase in concentration of inhibitor in catholyte. For example, a value of $t_0 = 416$ hours was determined in Figure 2b at the crossing of the two straight lines that represent the two transport stages of the TBA-B inhibitor. Following the same procedure the D of TMA-C was also determined.

$$D = \frac{dRT}{t_0 EzF} \qquad (1)$$

Where d = thickness of concrete disc, 2×10^{-2} m;

t_0 = the time required for inhibitor ions to penetrate a depth d;

E = electric field (the gradient of the potential), 600V/m (12V/0.02m);

z = electric charge carried by the organic cation, 1;

Values of $R, T,$ and F are listed in Table 4.

Based on the results of the electro-migration tests, the apparent diffusion coefficient D of TBA-B, TMA-C, and chloride ions were measured to be 1.2×10^{-11} m²/s, 1.75×10^{-11} m²/s, and 9.62×10^{-11} m²/s, respectively. In determining the D value of chloride ions, the same device as shown in Figure 1 was used. In this case, 200mM sodium chloride and 200mM sodium nitrate were added in the left and right compartments respectively to ensure similar conductivity on two sides of the concrete disc. The chloride concentration was measured directly from the destination solution using a custom-made Ag/AgCl chloride sensor.

Table 4: Input Parameters for FEM Analysis

Parameter	Physical Meaning	Value
i_0	externally applied cathodic current density	1, 3, 5 A/m²
F	Faraday's constant	9.64846×10^4 C/mol
R	ideal gas constant	8.3143 J/(mol·K)
T	absolute temperature	298.15 K (= 25 °C)
α_{Cl-}	Langmuir isotherm parameter for Cl⁻	1.63
β_{Cl-}	Langmuir isotherm parameter for Cl⁻	4.12×10^{-3} m³/mol
α_{TBA+}	Langmuir isotherm parameter for TBA⁺	0.1
β_{TBA+}	Langmuir isotherm parameter for TBA⁺	2.35×10^{-3} m³/mol
α_{TMA+}	Langmuir isotherm parameter for TMA⁺	0.1
β_{TMA+}	Langmuir isotherm parameter for TMA⁺	3.91×10^{-3} m³/mol

Finite Element Method Modeling

A 2D Finite Element Method (FEM) model recently developed in our laboratory [21] was used in this study to predict the concentration evolution of various species including mainly the inhibitor, chloride and hydroxyl ions in concrete (including rebar surface). It is capable of simulating the concurrent transport behavior of multiple ionic species in concrete under an externally applied electrical field.

This FEM model was developed based on the mass balance equation of ionic species in an electrolyte such as the concrete pore solution. As shown in Equation 1, C_i denotes the concentration of free species i in the electrolyte; J_i is the mass transport flux of species i. r_i is the production rate of species i that takes a value of zero when no new material of species i is generated.

$$\frac{\partial C_i}{\partial t} = -\nabla \cdot J_i - r_i, \quad i = 1, 2, 3, ... n, \tag{1}$$

As shown in Equation 2, J_i considers the two main mechanisms of species transport in a saturated concrete: natural diffusion and electric migration.

$$J_i = -D_i(\nabla C_i) - z_i \frac{D_i F}{RT} C_i (\nabla \phi) \tag{2}$$

In addition to the laboratory-determined D values of chloride ions and the inhibitors, the FEM analysis also needed the D values of other species including mainly the sodium, potassium and hydroxyl

ions. The D values of these species, however, are not so sensitive to the concrete ingredients and were obtained from literature [23]: 2.66×10^{-11}, 3.92×10^{-11}, and 1.01×10^{-10} for Na$^+$, K$^+$ and OH$^-$ respectively.

$$C_{bi} = \frac{\alpha \cdot C_{fi}}{1 + \beta \cdot C_{fi}} \qquad (3)$$

The 2D FEM model considers the binding of chloride and inhibitor ions with cement hydration products using a Langmuir Isotherm (see Equation 3) to describe the relationship between the concentration of bound species i (C_{bi}) and that of free species i (C_{fi}) [22]. The α and β parameters of chloride ions were determined using the concrete discs subsequent to the electro-migration tests. The 2-cm concrete discs were cut into three thinner slices with equal thickness. Each slice cut into four pieces, and each piece was then ground to powder. The powder samples were then boiled in water or nitric acid, in order to determine the free and total chloride concentrations respectively, following the Florida methods [24]. Following the same procedure the α and β parameters of TBA-B and TMA-C was also determined and all the results are presented in Table 4.

Considering the binding of species, the governing equation of species transport in concrete can be ultimately formulated as Equation 4. Details about the FEM model are presented in reference [21].

$$\frac{\partial C_{fi}}{\partial t} + \frac{\partial C_{bi}}{\partial t} = \nabla \cdot D_i (\nabla C_{fi}) + \nabla \cdot [z_i \frac{D_i F}{RT} C_{fi} (\nabla \cdot \phi)], \quad i = 1, 2, 3, ...m, \qquad (4)$$

The 2D FEM model was validated by comparing the experimentally measured chloride and inhibitor concentration profiles of the 2-cm concrete discs (as obtained using titration technique subsequent to the electro-migration tests) to their FEM predictions based on the measured D values. It was found that the concentration difference between the FEM prediction and the laboratory measurement was within 10% all over the specimen, which might be attributable to experimental errors.

FEM Analysis of Species Distributions after EICI

A 2D concrete domain of the 0.1207 m × 0.0762 m (4.75 in. × 3 in.) was evaluated using the FEM model. A steel rebar with a 0.0191 m (3/4 in.) diameter served as the cathode passing through the centroid of the concrete domain. The thickness of the concrete that covered the rebar was 0.0508 m (2 in.), which was intended to represent the lower boundary of typical concrete structures in chloride-laden environments. The geometry of the concrete domain and rebar position are given in Figure 3. To make use of the laboratory determined D values and α and β parameters, the virtual 2D concrete domain was assumed to have the same mixture design as the specimens used in the electro-migration tests.
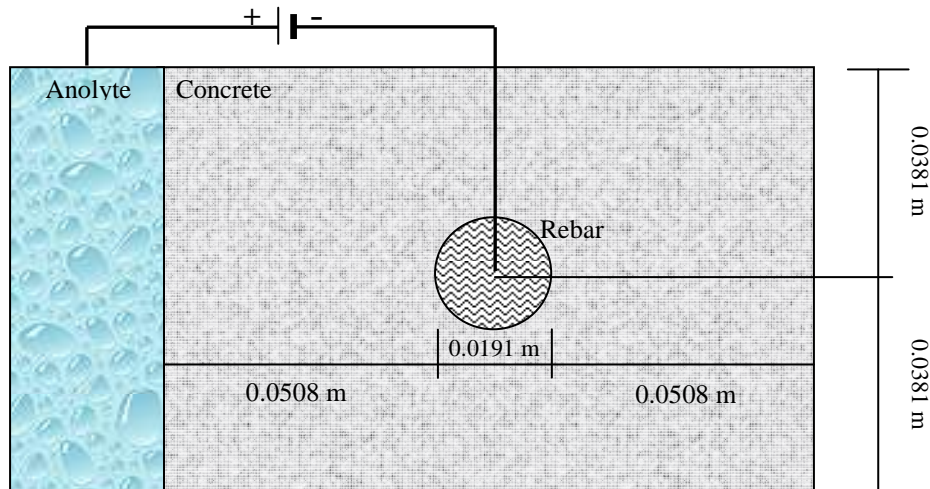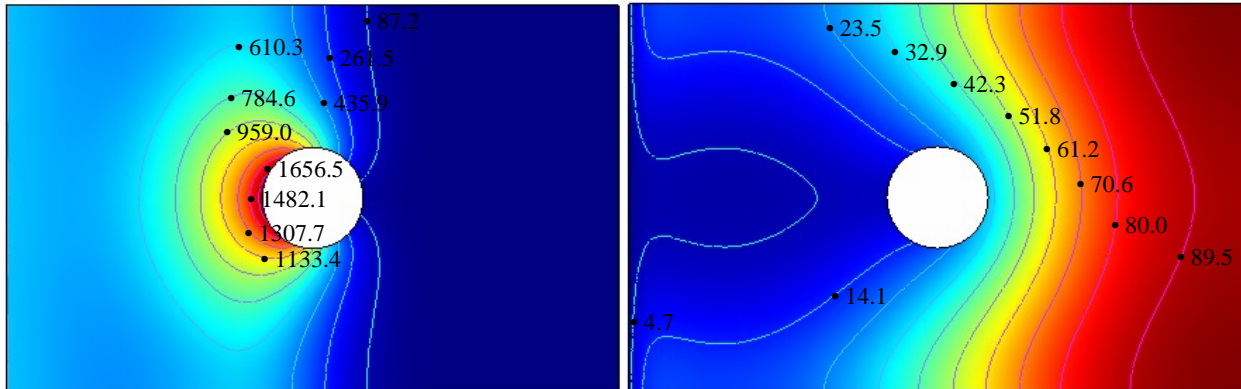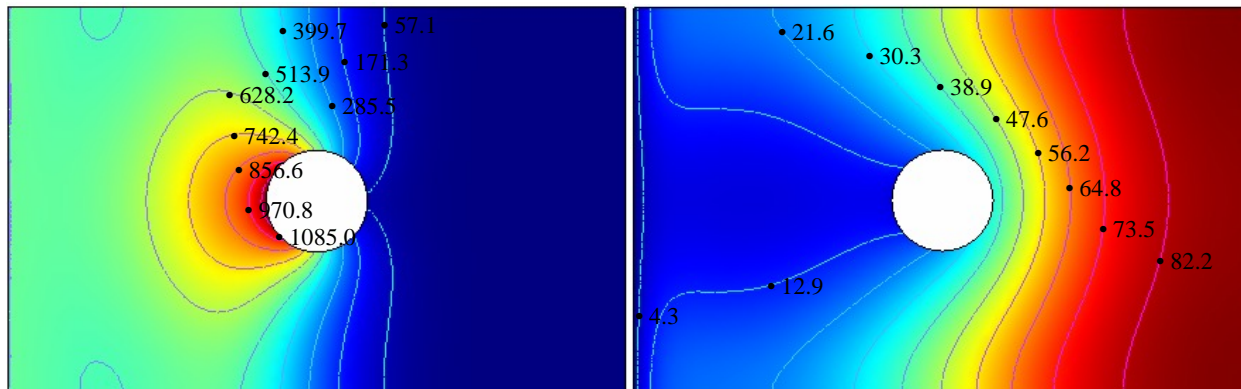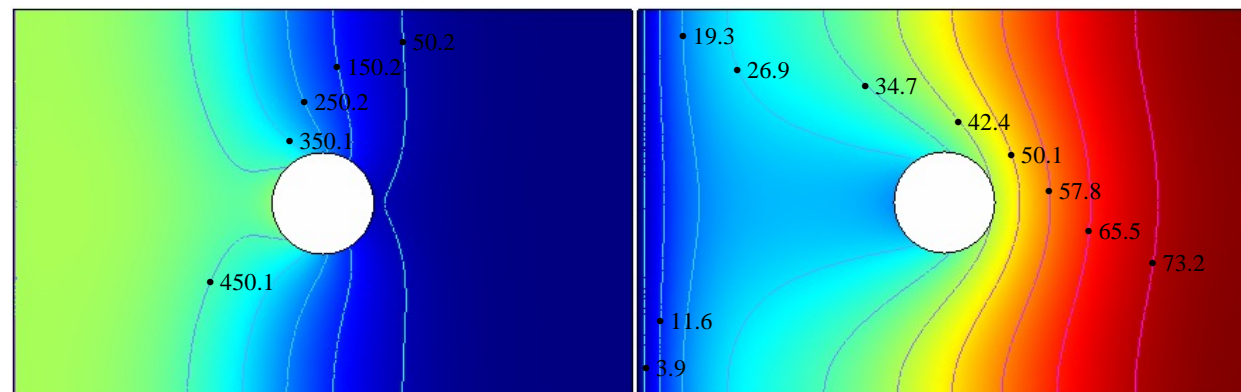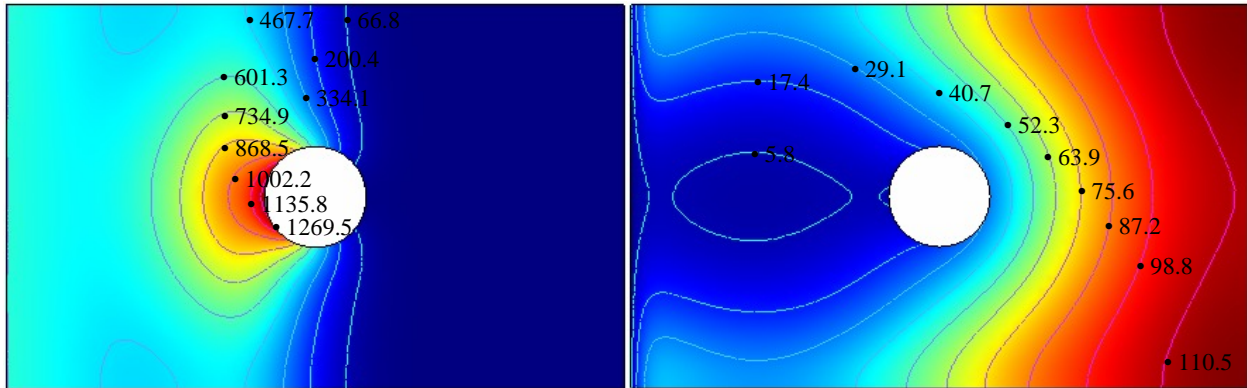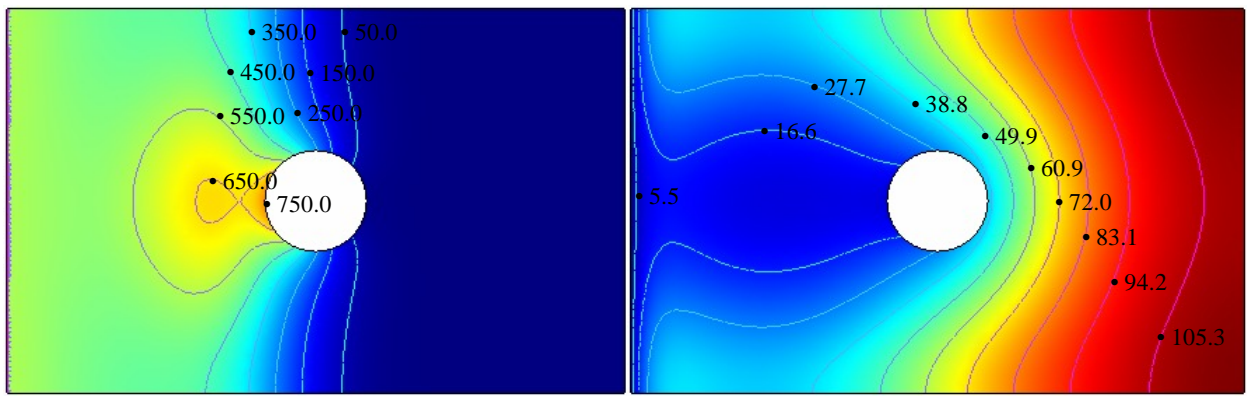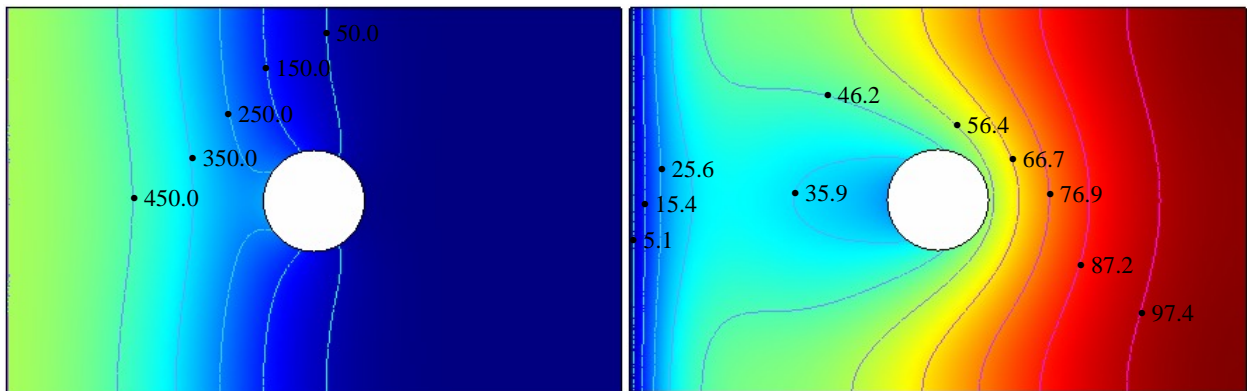

Figure 3: Schematic Illustration of the 2D Concrete Domain for FEM Analysis

For the FEM analysis, the cathodic current density i_0 was applied directly as boundary condition. Three levels of current density, i.e., 1 A/m², 3 A/m² and 5 A/m² were evaluated to find an appropriate level for effectively driving the inhibitor. The initial concentrations of various ionic species in concrete were assumed as follows: $[Cl^-]_{total}$ = 513 mM, $[OH^-]$ = 100 mM (or pH 13 to simulate typical hydrated cement concrete), $[In^+]$ = 0 mM, $[Na^+]$ = 513 mM, and $[K^+]$ = 100 mM. The sodium chloride concentration of 513 mM intended to simulate a contaminated concrete containing 3% of NaCl by weight of the pore solution. The left-hand side boundary in Figure 3 was next to the running anolyte solution that maintained a constant concentration for all the species, following the Dirichlet boundary conditions, i.e., $[C_i]$ = $[C_i]_{anolyte}$. In the anolyte, the concentrations of these species were maintained as: $[Cl^-]_{anolyte}$ = 0 mM, $[OH^-]_{anolyte}$ = 400 mM, $[Na^+]_{anolyte}$ = 400 mM, $[In^+]_{anolyte}$ = 1000 mM, and $[K^+]_{anolyte}$ = 0 mM.

(a) 5 A/m² after 16 Weeks

(b) 3 A/m² after 23 Weeks

(c) 1 A/m² after 46.7 Weeks

Figure 4: Concentration Profiles of TBA$^+$ (left) and Cl$^-$ (right) after EICI (mM)

(a) 5 A/m^2 after 8.9 Weeks

(b) 3 A/m^2 after 12.3 Weeks

(c) 1 A/m^2 after 22.2 Weeks

Figure 5: The Concentration Profiles of TMA$^+$ (left) and Cl$^-$ (right) after EICI (mM)

The electrical potential on the left-hand side boundary was set at zero, i.e., $\phi = 0$ as the reference potential. The Neumann boundary condition with flux equal to zero were applied to the top, bottom and right-hand side boundaries for all the five species and the electric current, i.e., $J_i = 0$, and $I_x = I_y = 0$, assuming no species could pass these boundaries. On the boundary at rebar surface, the zero concentration Dirichlet boundary condition was applied for the species Cl$^-$, Na$^+$, K$^+$, and the inhibitor. The Neumann boundary conditions were applied for the OH$^-$ on rebar surface, based on the assumption that externally supplied current flux is maintained by generating a constant hydroxyl flux on the rebar surface, i.e., $J_{OH^-} = i_0/Fz_{OH^-}$.
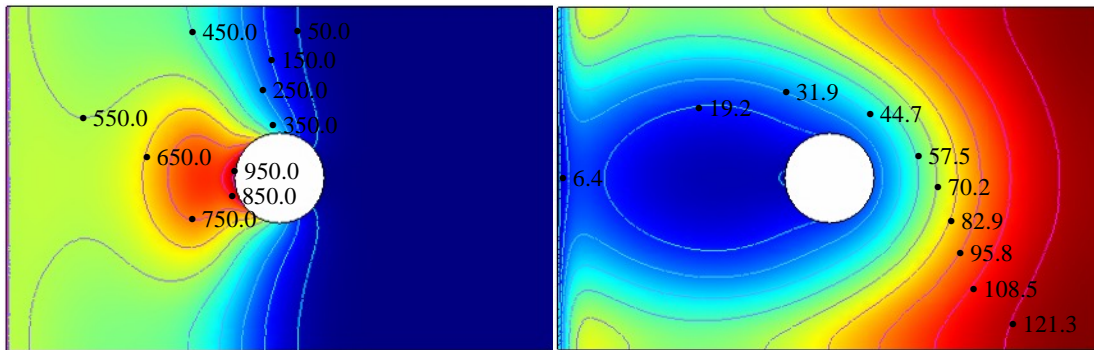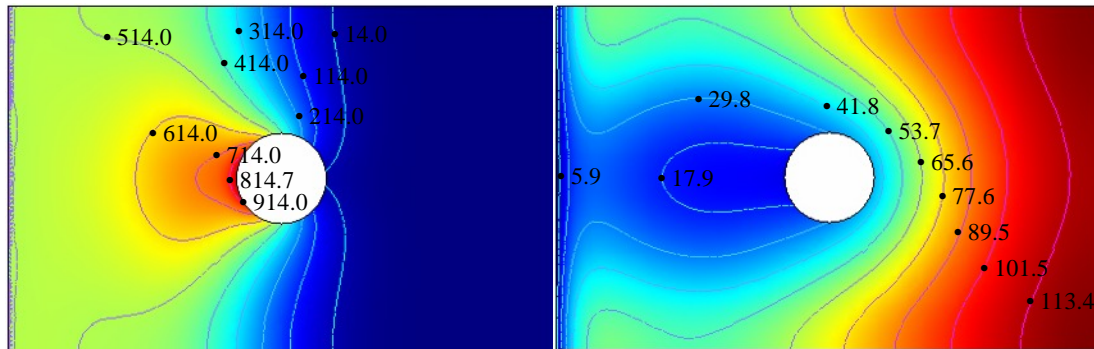
In EICI, while the inhibitor cations are driven to the rebar surface and the chloride ions are removed from the concrete, hydroxyl ions are also generated on the rebar surface and increase the pH value in the vicinity of rebar. Figures 4 and 5 present the concentration profiles of the TBA^+ and TMA^+ respectively, in which the concentration profiles of Cl^- as a result of EICI were also included. Based on the model prediction, none of the species Cl^-, TBA^+ and TMA^+ has a uniform concentration distribution on the rebar surface after EICI, whereas hydroxyls distribute uniformly around the rebar surface resulting in pH values close to 14. The non-uniform distributions of chloride and inhibitor ions on the rebar surface make it difficult to evaluate the effectiveness of EICI treatment.

The objective of the FEM analysis was to determine and evaluate the time needed for sufficient inhibitor to reach the rebar surface driven by an applied electric field. In this study, a conservative criterion was used by examining the concentrations of the chloride and inhibitor ions at the critical location on the rebar surface that is farthest from the anolyte pond. Figure 4a shows that a 5 A/m^2, 16-week EICI treatment resulted in a 54 mM TBA^+ concentration and a 29 mM free Cl^- concentration at the critical location. To reach the same 54 mM TBA^+ concentration at the critical location (which corresponds to a relatively good inhibition efficiency of TBA-B at pH 13 and Cl^- concentrations of 66 and 133 mM as shown in Table 3), the treatment time under an electric field of 3 A/m^2 and 1 A/m^2 would be increased to 23 weeks and 46.7 weeks, respectively, as shown in Figure 4b and Figure 4c.

Figures 5a-c provide the concentration profiles of the chloride and inhibitor ions in concrete after EICI, using the inhibitor (TMA-C) with a diffusion coefficient about 46 percent higher than TBA-B. For TMA-C, an inhibitor concentration of 10 mM (significantly lower than 54 mM in the case of TBA-B) corresponds to relatively good inhibition efficiency at pH 13 and Cl^- concentrations of 66 and 133 mM as shown in Table 3. To reach similar level of inhibition effectiveness at the critical location on the rebar surface, the treatment time of EICI was halved when switching from TBA-B to TMA-C, attributable to both the faster transport speed of TMA-C in concrete and its better inhibition efficiency. Figure 5a shows that a 5 A/m^2, 8.9-week EICI treatment resulted in a 10 mM TMA^+ concentration and a 29 mM free Cl^- concentration at the critical location. To reach the same 10 mM TMA^+ concentration at the critical location, the treatment time under an electric field of 3 A/m^2 and 1 A/m^2 would be increased to 12.3 weeks and 22.2 weeks, respectively, as shown in Figure 5b and Figure 5c.

To further elucidate the effect of D value on the treatment time required to reach similar level of inhibition effectiveness on the rebar surface, we examined the case of using the Proprietary Inhibitor for EICI, which had a diffusion coefficient about 70 percent higher than TMA-C and inhibition efficiency similar to TMA-C. The treatment time of EICI was further reduced by approximately 40 percent when switching from TMA-C to the Proprietary Inhibitor, attributable to the faster transport speed of the inhibitor in concrete ($D = 2.98 \times 10^{-11}$ m^2/s). Figure 6a shows that a 5 A/m^2, 5.2-week EICI treatment resulted in a 10 mM PI^+ concentration and a 29 mM free Cl^- concentration at the critical location. To reach the same 10 mM PI^+ concentration at the critical location, the treatment time under an electric field of 3 A/m^2 would be increased to 7 weeks, as shown in Figure 6b.

In reality, subsequent to the EICI process, both the aggressive species (Cl^-) and protective species (OH^- and PI^+) will re-migrate in concrete as a result of their non-uniform distributions in concrete, which is the subject of another FEM model being developed at our laboratory. Take Figure 6b as an example, after the applied electric field is removed, even though the pH value around the rebar surface will eventually decrease to closer to 13 and on the rebar surface the free Cl^- concentration will increase to higher than 30 mM as free Cl^- ions are either released from bound chloride in concrete or diffused from high-concentration locations in concrete, the inhibitor PI^+ concentration will increase to much higher than 10 mM on the rebar surface. Therefore, for field practice of EICI on the structure with 2-inch-thick concrete cover, much less treatment time than 7 weeks is necessary for driving sufficient PI^+ to the rebar surface when a current density of 3 A/m^2 is used. It is generally accepted that an externally applied current density lower than 5 A/m^2 would not incur significant damage to concrete matrix or side reactions. As such, the FEM analysis confirms that when an appropriate corrosion inhibitor is utilized, it is feasible to electrically inject sufficient amount of inhibitor into salt-contaminated concrete within a reasonable time frame (to minimize maintenance efforts and disruption to traffic).

(a) 5 A/m^2 after 5.2 Weeks

(b) 3 A/m^2 after 7 Weeks

Figure 6: The Concentration Profiles of PI$^+$ (left) and Cl$^-$ (right) after EICI (mM)

Conclusions, Recommendations and Limitations

This research aimed to assess the potential applicability of EICI as a routine electrochemical treatment for corrosion protection. First of all, the inhibition efficiency of eight organic chemicals was evaluated as potential corrosion inhibitors, by monitoring the corrosion rate of steel in a very aggressive, simulated concrete pore solution in presence of each inhibitor at 20 mM. The data show that tetrabutylammonium bromide (TBA-B) and tetramethylammonium chloride (TMA-C) outperformed other chemicals as corrosion inhibitors in the simulated concrete pore solution, by reducing the corrosion rate of steel by 85 percent and 75 percent, respectively. More laboratory tests were conducted to further investigate the performance of TBA-B and TMA-C in less aggressive environments representative of concrete with less chloride contamination or with reduce chloride content through electrochemical treatment. The data indicate that TMA-C outperformed TBA-B as corrosion inhibitor in the less aggressive environments. Generally the corrosion of steel was less severe in simulated concrete pore solutions with a lower chloride concentration (66 mM vs. 133 mM), or with a higher inhibitor concentration (50 mM vs. 5 mM and 0 mM).

Secondly, the apparent diffusion coefficients (*D*) of chloride and organic cations were measured in this study using electrically-accelerated migration tests. The *D* values of TBA-B, TMA-C, and chloride ions were measured to be 1.2×10^{-11} m^2/s, 1.75×10^{-11} m^2/s, and 9.62×10^{-11} m^2/s, respectively.

Finally, a two-dimensional (2D) Finite Element Method (FEM) model recently developed in our laboratory was used in this study to predict the concentration evolution of various species including mainly the inhibitor, chloride and hydroxyl ions in concrete. Based on the model prediction, none of the species Cl$^-$, TBA$^+$ and TMA$^+$ has a uniform concentration distribution on the rebar surface after EICI, whereas hydroxyls distributes uniformly around the rebar surface resulting in pH values close to 14. The objective of the FEM analysis was to determine and evaluate the time needed for sufficient inhibitor to

reach the rebar surface driven by an applied electric field. In this study, a conservative criterion was used by examining the concentrations of the chloride and inhibitor ions at the critical location on the rebar surface that is farthest from the anolyte pond.

To reach a 54 mM TBA^+ concentration at the critical location (which corresponds to a relatively good inhibition efficiency of TBA-B at pH 13 and Cl^- concentrations of 66 and 133 mM), the treatment time under an electric field of 5 A/m^2, 3 A/m^2 and 1 A/m^2 would be 16 weeks, 23 weeks, and 46.7 weeks, respectively. To reach similar level of inhibition effectiveness at the critical location on the rebar surface, the treatment time of EICI was halved when switching from TBA-B to TMA-C, attributable to both the faster transport speed of TMA-C in concrete and its better inhibition efficiency. The treatment time of EICI was further reduced by approximately 40 percent when switching from TMA-C to the Proprietary Inhibitor, attributable to the faster transport speed of the inhibitor in concrete ($D = 2.98 \times 10^{-11}$ m^2/s).

In reality, subsequent to the EICI process, both the aggressive species (Cl^-) and protective species (OH^- and PI^+) will re-migrate in concrete as a result of their non-uniform distributions in concrete, which is the subject of another FEM model being developed at our laboratory. The analysis indicate that for field practice of EICI on the structure with 2-inch-thick concrete cover, much less treatment time than 7 weeks is necessary for driving sufficient PI^+ to the rebar surface when a current density of 3 A/m^2 is used.

For EICI, inhibitors that demonstrate satisfactory inhibition effectiveness, and equally importantly, that can also be electrically driven to the rebar surface in a short time are highly desired. Only the Proprietary Inhibitor we evaluated seem to allow practical application of EICI, whereas other chemicals evaluated either lacked high and consistent inhibition efficiency over time or did not have high transport speed in concrete. In the latter case, it would significantly extend the treatment time required to inject sufficient inhibitor to rebar surface and render the EICI practice infeasible. While increasing the magnitude of applied current density can help reduce the treatment time, it has to be maintained lower than 5 A/m^2 to avoid potential damage to concrete matrix or side reactions.

The selection of corrosion inhibitors is essential to the successful implementation of EICI practice as a rehabilitative measure for salt-contaminated concrete. The FEM analysis confirms that when an appropriate corrosion inhibitor is utilized, it is feasible to electrically inject sufficient amount of inhibitor into salt-contaminated concrete within a reasonable time frame (to minimize maintenance efforts and disruption to traffic). A good corrosion inhibitor for EICI should not only provide excellent effectiveness in mitigating chloride-induced corrosion of steel but also feature a high transport speed in concrete ($D \geq 2 \times 10^{-11}$ m^2/s). Design and synthesis of new molecules (such as the Proprietary Inhibitor) may be necessary to address these needs. A successful EICI treatment should also consider the structural and environmental issues, such as the thickness of the concrete cover, the position of rebar in the concrete structure, the susceptibility of aggregates to alkali-silica reactions (ASR), the alkalinity of the concrete, and the risk of carbonation and sulfate attack. All these factors can possibly affect the feasibility and performance of EICI.

Although the effectiveness of the inhibitors and the concentration profiles of chloride, inhibitors and hydroxyls in concrete can be precisely determined based on laboratory experiments and modeling, this study leaves two important issues unaddressed, i.e., the time required to form up a protective inhibitor film and the reliability of the inhibitor film after EICI. The laboratory section of this study focuses on a phenomenological evaluation of inhibitor performance without exploring the fundamentals of the inhibiting mechanism. Work is planned in our laboratory to examine these very issues, in an attempt to better understand the inhibition mechanism of organic cation-based inhibitors for chloride-induced corrosion of steel, the relationship between molecular structure and diffusion coefficient of inhibitors, the transport behavior and re-migration of species subsequent to EICI, the reliability of inhibitor film on rebar surface subsequent to EICI, etc. Such research would advance the knowledge base for the EICI practice and lead to more electrochemical rehabilitation of aging concrete structures.

Acknowledgements

like to extend our appreciation to Dr. Xiaodong He at our laboratory for his assistance in the early stage of this research.

References

[1] Cady, P.D., and Weyers, R.E., "Predicting service life of concrete bridge decks subject to reinforcement corrosion." *Corrosion Forms and Control for Infrastructure*, *ASTM Spec. Tech.* Publication No. 1137, pp. 328–338, 1992.

[2] Liam, K.C., Roy, S.K. and Northwood, D.O., "Chloride Ingress Measurements and Corrosion Potential Mapping of a 24 Year Old Reinforced Concrete Jetty Structure in a Tropic Marine Environment', *Magazine of Concrete Research*, Vol. 44, No. 160, 1992.

[3] Hartt, W. and Nam, J., "Critical Parameters for Corrosion Induced Deterioration of Marine Bridge Substructures in Florida," prepared for the Florida Department of Transportation, 2004.

[4] Pruckner, F. and Gjørv, O.E., "Effect of $CaCl_2$ and NaCl Additions on Concrete Corrosivity," *Cement and Concrete Research*, Volume 34, Issue 7, pp. 1209-1217, 2004.

[5] Buenfeld, N.R., Glass, G.K., Hassanein, A. M. and Zhang, Jian-Zhong, "Chloride Transport in Concrete Subjected to Electric Field," *Journal of Materials in Civil Engineering*, Vol. 10 No. 4, pp. 220-228, 1998.

[6] Ababneh, A., Benboudjema, F., and Xi, Y., "Chloride Penetration in Nonsaturated Concrete," *Journal of Materials in Civil Engineering, ASCE*, Vol. 15, No. 2, pp. 183-191, 2003.

[7] Al-Qadi I.L., Prowell, B.D., Weyers, R.E., Dutta, T., Gouru, H., and Berke, N., "Concrete Bridge Protection and Rehabilitation: Chemical and Physical Techniques - Corrosion Inhibitors and Polymers," SHRP-S-666. Strategic Highway Research Program. Washington, DC, 1993.

[8] Gaidis, J.M., "Chemistry of corrosion inhibitors," *Cement and Concrete Composites*, Volume 26, Issue 3, pp. 181-189, 2004.

[9] Johannesson B.F., "Diffusion of a Mixture of Cations and Anions Dissolved in Water - Effects on Pore Space Percolation and Diffusivity," *Cement and Concrete Research*, Volume 29, No. 8, pp. 1261-1270, 1999.

[10] Boulfiza, M., Sakai, K., Banthia, N. and Yoshida, H. "Prediction of Chloride Ions Ingress in Uncracked and Cracked Concrete," *ACI Materials Journal*, Vol. 100, pp. 38-48, 2003.

[11] Bennett, J.K., Fong, F., and Schue, T.J., "Electrochemical chloride removal and protection of concrete bridge components: field trials," *Report # SHRP S-669, Strategic Highway Research Program*, Washington, D.C., National Research Council. 1993.

[12] Sawada, S., Page, C.L. and Page, M.M., "Electrochemical Injection of Organic Corrosion Inhibitors into Concrete," *Corrosion Science*, Vol. 47, No. 88, pp. 2063-2078, 2005.

[13] NACE SP0107-2007, "Electrochemical Realkalization and Chloride Extraction for Reinforced Concrete," National Association of Corrosion Engineers (NACE), 2007

[14] Fajardo, G., and Escadeillas, A.G., "Electrochemical Chloride Extraction (ECE) from Steel-reinforced Concrete Specimens Contaminated by "Artificial" Sea-water," *Corrosion Science*, Vol. 48, pp. 110-125, 2006.

[15] Bennett, J.K., Schue, T.J., Clear, K.C., Lankard, D.L., Hartt, W.H. and Swiat, W.J., "Electrochemical chloride removal and protection of concrete bridge components: laboratory studies," *Report # SHRP S-657, Strategic Highway Research Program*, Washington, D.C., National Research Council. 1993.

[16] Hausmann, D.A. "A Probability Model of Steel Corrosion in Concrete," *Materials Performance*. Vol. 37, No. 10, pp. 64-68, 1998.

[17] Hartt, W.H., Charvin, S., and Lee, S., "Influence of Permeability Reducing and Corrosion Inhibiting Admixtures in Concrete upon Initiation of Salt Induced Embedded Metal Corrosion," prepared for the Florida Department of Transportation, 1999.

[18] Hettiarachchi, S., Gaynor, A.T., and Asaro, M.F., "Electrochemical Chloride Removal and Protection of Concrete Bridge Components (Injection of Synergistic Inhibitors)," SHRP-S-310. Strategic Highway Research Program, National Research Council, Washington D.C., 1987.

[19] Sawada, S., Page, C.L., and Page, M.M., "Electrochemical Injection of Organic Corrosion Inhibitors into Concrete," *Corrosion Science*, Vol. 47, pp.2063-2078, 2005.

[20] Bennett, G. E. and Johnston, K. P., "UV-visible Absorbance Spectroscopy of Organic Probes in Supercritical Water," *Journal of Physical Chemistry*, Vol. 98, pp. 441-447, 1994.

[21] Pan, T., Shi, X., and Nguyen, T. A., "Finite Element Modeling of Ionic Transport in Concrete under an Externally Applied Electric Field," Submitted to ASCE Journal of Materials in Civil Engineering.

[22] Pereira, C., and Hegedus, L., "Diffusion and Reaction of Chloride Ions in Porous Concrete", *Proceedings of the 8th International Symposium on Chemical Reaction Engineering*, Vol. 87, pp. 427-438, 1984.

[23] Yu, S., and Page, C.L. "Computer Simulation of Ionic Migration during Electrochemical Chloride Extraction from Hardened Concrete," *British Corrosion Journal*, Vol. 31, No.1, pp. 73-75, 1996.

[24] Florida Department of Transportation, Florida method of Test for Determining Low-Levels of Chloride in Concrete and Raw Materials. FM-5-516. 2000.